Weak ferrimagnetism, compensation point, and magnetization reversal in $Ni(HCOO)_2 \cdot 2H_2O$

H. Kageyama,[1] D. I. Khomskii,[2] R. Z. Levitin,[3] and A. N. Vasil'ev[1,*]

[1]*Materials Design and Characterization Laboratory, Institute for Solid State Physics, University of Tokyo, 5-1-5 Kashiwanoha, Kashiwa, Chiba 277-8581, Japan*

[2]*Solid State Physics Laboratory, Materials Science Center, University of Groningen, Nijenborgh 4, 9747 AG Groningen, The Netherlands*

[3]*Physics Faculty, Moscow State University, Moscow 119992, Russia*

(Received 28 October 2002; revised manuscript received 13 March 2003; published 18 June 2003)

The nickel (II) formate dihydrate $Ni(HCOO)_2 \cdot 2H_2O$ shows a peculiar magnetic response at $T < T_N = 15.5$ K. The magnitude of the weak magnetic moment increases initially below T_N, is zero at $T^* = 8.5$ K, and increases again at lowered temperature. The sign of low-field magnetization at any given temperature is determined by the sample's magnetic prehistory and the signs are opposite from each other at $T < T^*$ and $T^* < T < T_N$. This behavior suggests that $Ni(HCOO)_2 \cdot 2H_2O$ is a weak ferrimagnet and T^* is a compensation point. The magnetic properties of $Ni(HCOO)_2 \cdot 2H_2O$ can be understood by taking into account the features of its crystal structure. There are two nonequivalent Ni sites in the monoclinic $P2_1/c$ structure of this compound, forming two magnetic subsystems. Each of these subsystems is weakly ferromagnetic due to the canting of predominantly antiferromagnetic sublattices. The weak ferromagnetic moments of these subsystems are oriented opposite from each other, resulting in weak ferrimagnetism. The model proposed explains the main features of the experimentally observed phenomena.

DOI: 10.1103/PhysRevB.67.224422 PACS number(s): 75.30.−m, 75.50.−y, 75.60.−d

I. INTRODUCTION

The phenomenon of ferrimagnetism is associated with a partial cancellation of antiferromagnetically aligned magnetic sublattices with different values of magnetic moments and/or different temperature dependencies of magnetization. It has been well studied in ferrites[1,2] and recently in various inorganic[3,4] and molecular transition-metal complexes.[5–10] Ferrimagnetic behavior is observed frequently in compounds containing different magnetic ions. It can also be seen in materials containing only one type of magnetic ions but with either different valence states or different crystallographic positions.[11,12] In the latter case the origin of ferrimagnetism lies in the difference of molecular fields acting on nonequivalent magnetic sites.

In some ferrimagnets (according to the Néel's classification, it is *N*-type ferrimagnets[13]) the total magnetization of a substance becomes zero at a certain compensation temperature T^*. Both above and below this temperature the magnetization of different sublattices prevails. In this case magnetization reversal can be observed. In weak magnetic field (less than the field of coercivity) the magnetization changes sign at the compensation temperature. The metastable ''diamagnetic'' state at a certain temperature range can be fixed by magnetocrystalline anisotropy.[2]

Much rarer is the observation of magnetization reversal in canted antiferromagnets, where the weak ferromagnetic moment is due to the tilting of sublattice magnetizations. The single-ion magnetic anisotropy itself can fix the directions of sublattice magnetizations tilted from antiparallel alignment.[14] On other hand, the canting of antiferromagnetic sublattices can be due to antisymmetric Dzyaloshinsky-Moriya interaction,[15–17] which favors perpendicular orientations of the sublattice magnetizations. Very few canted antiferromagnets show compensation point and magnetization reversal. These phenomena were observed in YVO_3 single crystals and were treated on the basis of competition between the single-ion anisotropy and Dzyaloshinsky-Moriya interaction.[18,19] In orthoferrites $Y(FeCr)O_3$ the ferrimagneticlike behavior and compensation point were ascribed to competition of the Dzyaloshinsky-Moriya interactions between different magnetic ions.[20]

Herein, we report the observation of weak ferrimagnetism, compensation point, and magnetization reversal in the nickel (II) formate dihydrate $Ni(HCOO)_2 \cdot 2H_2O$. The magnetic and thermal properties of isostructural dihydrated formates of transition metals were extensively studied in the 1970s. The interest was due to the specific layered arrangement of metal ions in the crystal structure of these compounds. Within layers the metal ions are either linked by formate groups or they are not. This alternate stacking of coupled and uncoupled metal ions suggested the reduced dimensionality of the magnetic subsystem. The interlayer interaction through the formate groups was taken into account also, but was considered to be much weaker than the intralayer one. The predominantly antiferromagnetic ordering at Néel temperature $T_N = 3.72$ K in $Mn(HCOO)_2 \cdot 2H_2O$,[21–24] at $T_N = 3.74$ K in $Fe(HCOO)_2 \cdot 2H_2O$,[24–27] at $T_N = 5.1$ K in $Co(HCOO)_2 \cdot 2H_2O$,[24] and at $T_N = 15.5$ K in $Ni(HCOO)_2 \cdot 2H_2O$ (Refs. 24,25, and 27) was established. In the Ni-based formate long-range ordering was suggested to occur only within strongly coupled layers at T_N, while the metal ions in neighboring layers were considered to remain essentially independent even at low temperatures.[25] It was suggested[24] that the metal ions within magnetically coupled layers were set into canted antiferromagnetic states below T_N. It was argued,[27] however, that either ferrimagnetism or weak ferromagnetism of the canted antiferromagnet could be responsible for the spontaneous moment at low temperatures. Either of these situations is compatible with the crystal structure of dihydrated formates but the origin of the spontaneous moment in Mn- and Fe-based formates remains unclear. It

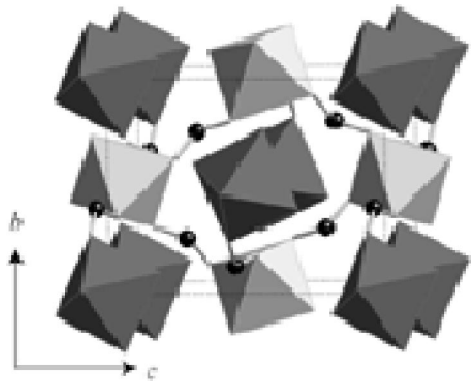

FIG. 1. The crystal structure of $Ni(HCOO)_2 \cdot 2H_2O$ in polyhedral representation. The octahedrons NiO_6 belonging to Ni_1 and Ni_2 subsystems are of light and dark shades, respectively. Note that each subsystem contains two kinds of octahedrons tilted with respect to each other. The dark circles denote the C ions, while the H ions are not shown for clarity. The solid lines indicate the exchange interaction links between Ni ions.

was not established explicitly whether the Ni-based formate possesses a nonzero moment below T_N.

This paper is organized in the following manner. First, the crystal structure of $Ni(HCOO)_2 \cdot 2H_2O$ is described. Then, the results of magnetization are presented and it is concluded that this compound is a weak ferrimagnet. A model of the magnetic structure of nickel formate dihydrate is suggested and a molecular-field theory for this model is given. A comparison of the results of calculation with experimental data and a discussion are provided.

II. CRYSTAL STRUCTURE

$Ni(HCOO)_2 \cdot 2H_2O$ crystallizes in the monoclinic $P2_1/c$ space group and includes 4 f.u. in the unit cell with $a = 0.860$ nm, $b = 0.706$ nm, $c = 0.921$ nm, and $\beta = 96.5°$.[22] It is of light blue color and presumably insulating. The structure, shown in Fig. 1, contains two kinds of Ni^{2+} ions: the Ni_1 with six oxygen atoms of different formate ions as nearest neighbors, the Ni_2 with four water molecules, and two formate oxygen atoms coordinated. In both Ni_1 and Ni_2 subsystems the octahedrons coordinating the Ni ions are tilted with respect to each other. The fourfold axes of NiO_6 octahedrons are oriented differently with respect to the crystal lattice axes. In the Ni_1 subsystem the fourfold axes lie mainly in the a-b crystal plane and are tilted for $\psi_1/2 = 22.5°$ in opposite directions from the a axis. In the Ni_2 subsystem the fourfold axes also lie mainly in the a-b plane and are tilted for $\psi_2/2 = 57.5°$ from the a axis. The slight deviations of NiO_6 fourfold axes from the a-b plane will be taken into account below.

III. EXPERIMENT

Magnetic properties of commercially available (Waco Company) powder samples of $Ni(HCOO)_2 \cdot 2H_2O$ were measured by the Quantum Design superconducting quantum interference device magnetometer in a 2–300-K temperature range up to 5 T. X-ray analysis confirmed the single phase of the title compound in the measured sample.

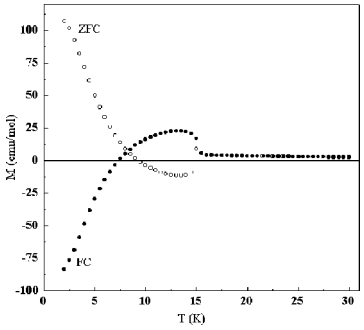

FIG. 2. The temperature dependencies of magnetization of $Ni(HCOO)_2 \cdot 2H_2O$ at $H = 0.01$ T taken in zero-field-cooling and field-cooling regimes.

The temperature dependencies of magnetization of the $Ni(HCOO)_2 \cdot 2H_2O$ powder sample taken in zero-field-cooling (ZFC) and field-cooling (FC) regimes at $H = 0.01$ T are shown in Fig. 2. At heating in the ZFC regime the sample shows first a large ''paramagnetic'' response at low temperatures, then the magnetic moment gradually decreases with increasing temperature, changes to ''diamagnetic'' at $T^* = 8.5$ K, and once again becomes paramagnetic above 15.5 K. At subsequent cooling in the FC regime the magnetic behavior of the sample at low temperatures appears to be mirrorlike with respect to magnetization sign as compared with ZFC measurements. The magnetization reversal was observed only at low magnetic field. At higher fields the magnetic moment monotonously increases at lowering temperature, showing only weak singularity at 15.5 K. This is in complete accordance with earlier observations.[25]

The M vs H curves in the range 2–15 K are shown in Fig. 3. These curves are ferromagneticlike, i.e., they show a spontaneous magnetic moment. The temperature dependence of the spontaneous magnetic moment of $Ni(HCOO)_2 \cdot 2H_2O$ is shown in Fig. 4. The saturation magnetization at low temperatures is two orders-of-magnitude smaller than that corresponding to the parallel alignment of Ni^{2+} magnetic moments. The ferromagneticlike character of the curves shown is supported by hysteretic behavior of magnetization. The

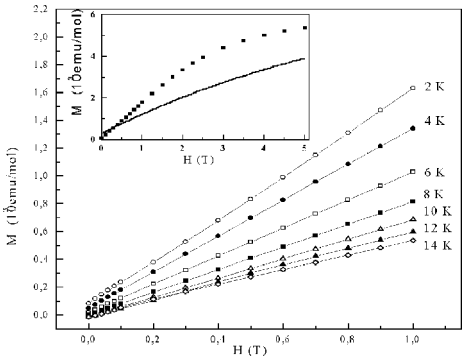

FIG. 3. The magnetization curves of $Ni(HCOO)_2 \cdot 2H_2O$. The inset shows theoretical (solid line) and experimental ($\diamond$) M vs H dependencies at $T = 2$ K.

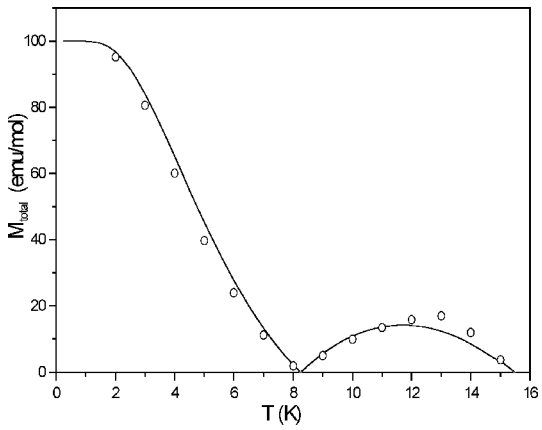

FIG. 4. The experimental (○) and theoretical (solid line) temperature dependencies of the spontaneous magnetic moment of $Ni(HCOO)_2 \cdot 2H_2O$.

magnetization loops of $Ni(HCOO)_2 \cdot 2H_2O$ taken at several temperatures are shown in Fig. 5, and the low-field region is enlarged in Fig. 6. Evidently, the remanent magnetization decreases with increasing temperature, is close to zero in vicinity of T^*, increases again at increasing temperature, and vanishes above 15.5 K.

Therefore, the experimental data presented suggest that below $T_N = 15.5$ K a weakly ferrimagnetic state in $Ni(HCOO)_2 \cdot 2H_2O$ is realized, and $T^* = 8.5$ K is a compensation temperature. The temperature dependence of high-field magnetic susceptibility χ in the magnetically ordered state obtained from the slope of magnetization curves at $H \sim 1$ T is shown in Fig. 7. This dependence is quite unusual for magnetically ordered compounds, i.e., χ increases at decreasing temperature.

The paramagnetic susceptibility χ_{para} of $Ni(HCOO)_2 \cdot 2H_2O$ was measured in a wide range from the Néel point to room temperature. At high temperatures χ_{para} follows the Curie-Weiss law with paramagnetic Curie temperature $\Theta = -15.5$ K and an effective magnetic moment $\mu_{eff} = 3.14\mu_B$. An experimental value of μ_{eff} is a typical one for Ni^{2+} ions in various compounds and exceeds the spin only part $2.82\mu_B$. This means that the orbital moment is not completely quenched in a crystal field. A negative value of Θ implies that the main exchange interaction in $Ni(HCOO)_2 \cdot 2H_2O$ is antiferromagnetic. When approaching T_N, the χ_{para} deviates from the Curie-Weiss law as shown in Fig. 8.

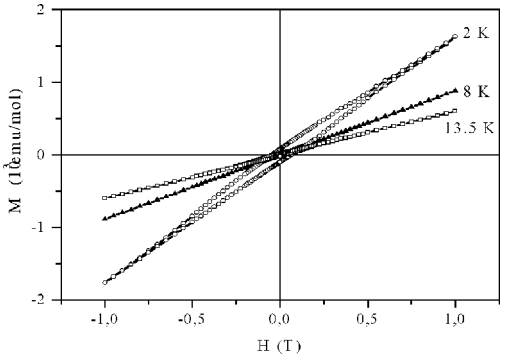

FIG. 5. The magnetization loops of $Ni(HCOO)_2 \cdot 2H_2O$ taken at various temperatures at $T < T_N$.

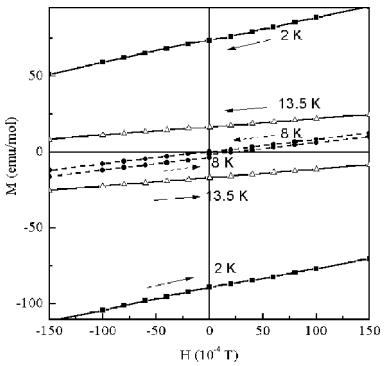

FIG. 6. The low-field regions of hysteresis loops of $Ni(HCOO)_2 \cdot 2H_2O$ taken at various temperatures at $T < T_N$.

IV. MODEL

The crystal structure considerations indicate that the superexchange pathways between Ni ions can be realized through Ni–O–C–O–Ni links. As noted earlier, both Ni_1 and Ni_2 subsystems contain two kinds of Ni ions with different orientations of octahedral environments. Consequently, it is natural to represent each Ni subsystem as consisting of two sublattices, namely, $Ni_{1'}$, $Ni_{1''}$ and $Ni_{2'}$, $Ni_{2''}$. The superexchange Ni–O–C–O–Ni links exist between $Ni_{1'}$ and $Ni_{1''}$ and also between $Ni_{1'}$ and $Ni_{2'}$, and $Ni_{1''}$ and $Ni_{2''}$. Therefore, each $Ni_{1'}$ ion interacts with four-nearest-neighboring $Ni_{1''}$ ions and two-nearest-neighboring $Ni_{2'}$ ions. The same is true for $Ni_{1''}$ ions. There is no Ni–O–C–O–Ni superexchange pathway within the Ni_2 subsystem. This means that in the absence of Ni_1 - Ni_2 exchange interactions the Ni_2 subsystem can be considered paramagnetic. The same exchange interactions pattern was used to analyze the magnetic properties of $Ni(HCOO)_2 \cdot 2H_2O$ in Ref. 24. Within Ni–O–C–O–Ni links the angles of superexchange interaction lie in the range $122° - 137°$, suggesting the predominance of antiferromagnetic interaction.[28,29] The param-

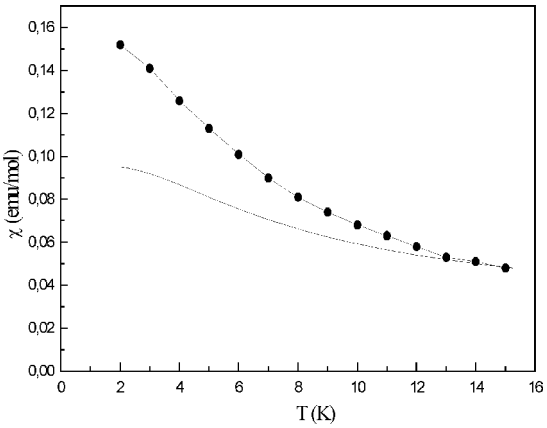

FIG. 7. The experimental (line+symbol) and theoretical (solid line) temperature dependencies of high-field magnetic susceptibility of $Ni(HCOO)_2 \cdot 2H_2O$ at $T < T_N$.

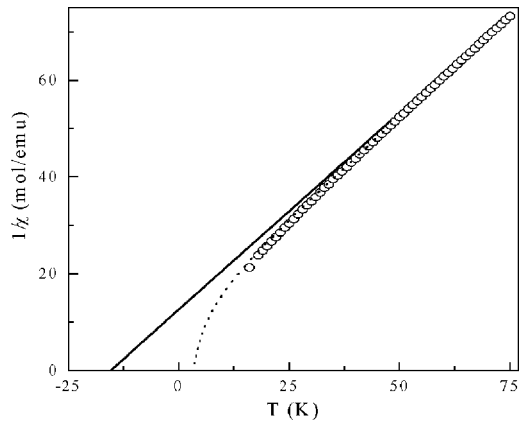

FIG. 8. The inverse paramagnetic susceptibility of $Ni(HCOO)_2 \cdot 2H_2O$ at $T > T_N$. The experimental data are shown by symbols. The solid line represents the Curie-Weiss law. The dotted line represents the results of calculation by Eq. (11).

eters of different pathways, i.e., angles and interatomic distances, are close to each other. In the first approximation the exchange interactions through these links can be considered equal. This approximation significantly simplifies the description of magnetic properties of $Ni(HCOO)_2 \cdot 2H_2O$, but is not critical. The magnetic structure corresponding to the pattern of exchange interactions described is shown in Fig. 9. The superexchange pathways are shown by solid lines. This structure is drawn in simplest exchange approximation and does not take into account the crystal-field effects leading to the single-ion anisotropy. The crystal-field effects fix the orientations of different Ni magnetic moments in different directions with respect to crystallographic axes and result in tilting of these moments from antiparallel alignment. The model suggested is oversimplified in the sense that it assumes a unique exchange interaction parameter within the magnetic system of $Ni(HCOO)_2 \cdot 2H_2O$. Another assumption is that the principal axes of NiO_6 octahedrons lie in the *a*-*b* plane and the model neglects their slight deviations from

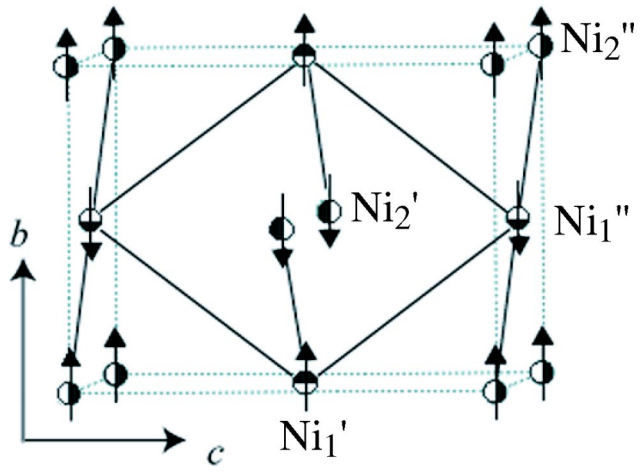

FIG. 9. The proposed magnetic structure of $Ni(HCOO)_2 \cdot 2H_2O$. The pathways of exchange interaction are shown by solid lines. The Ni ions belonging to two different sublattices within both Ni_1 and Ni_2 subsystems are represented by four different symbols.

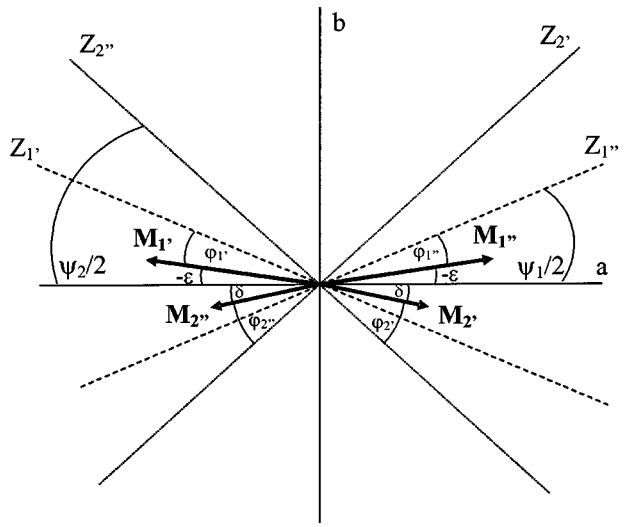

FIG. 10. The model of the weak ferrimagnetic structure of $Ni(HCOO)_2 \cdot 2H_2O$. The magnetic moments $M_{1'}$, $M_{1''}$, $M_{2'}$, and $M_{2''}$ of different Ni ions are assumed to lie in the *a*-*b* plane. The dotted lines show the orientations of the principal axes (easy directions of magnetization) $Z_{1'}$, $Z_{1''}$, $Z_{2'}$, and $Z_{2''}$ of different NiO_6 octahedrons. The angles between easy directions of magnetization and the *a* axis are $\psi_{1'}/2 = \psi_{1''}/2 = \psi_1/2$ and $\psi_{2'}/2 = \psi_{2''}/2 = \psi_2/2$. The deviations from antiparallel alignment of magnetic moments within Ni_1 and Ni_2 subsystems are designated as ε and δ, correspondingly. The angles $\varphi_{1'} = \varphi_{1''} = \varphi_1$ and $\varphi_{2'} = \varphi_{2''} = \varphi_2$ give the deviations of corresponding magnetic moments from easy directions of magnetization.

this plane. The model does not take into account an antisymmetric Dzyaloshinsky - Moriya interaction, which can lead also to weak ferromagnetism.

The properties of $Ni(HCOO)_2 \cdot 2H_2O$ in the framework of the model suggested above can be described using the following expression for free energy:

$$E = 4\lambda \mathbf{M_{1'}} \mathbf{M_{1''}} + 2\lambda (\mathbf{M_{1'}} \mathbf{M_{2'}} + \mathbf{M_{1''}} \mathbf{M_{2''}}) + K_{Ni_1} \sin^2 \varphi_{1'} + K_{Ni_1} \sin^2 \varphi_{1''} + K_{Ni_2} \sin^2 \varphi_{2'} + K_{Ni_2} \sin^2 \varphi_{2''} - \mathbf{H}(\mathbf{M_{1'}} + \mathbf{M_{1''}} + \mathbf{M_{2'}} + \mathbf{M_{2''}}), \quad (1)$$

where $\lambda = Ig^2\mu_B^2$ is the molecular-field coefficient, I is the exchange interaction parameter, g is the g factor, and $|\mathbf{M_{1'}}| = |\mathbf{M_{1''}}| = M_1$ and $|\mathbf{M_{2'}}| = |\mathbf{M_{2''}}| = M_2$ are the magnetic moments of Ni_1 and Ni_2 sublattices. The first term in Eq. (1) describes the exchange interactions within the Ni_1 subsystem, and the second term describes the exchange interactions between Ni_1 and Ni_2 subsystems. The next four terms describe the energy of magnetic anisotropy. The K_{Ni_1} and K_{Ni_2} are constants of the single-ion magnetic anisotropy of different Ni subsystems. The angles $\varphi_{1'} = \varphi_{1''} = \varphi_1$ and $\varphi_{2'} = \varphi_{2''} = \varphi_2$ are the angles between the axes of anisotropy and magnetic moments of corresponding Ni ions (see Fig. 10). It is natural to assume that the axes of anisotropy coincide with the principal axes of NiO_6 octahedrons. The last term in Eq. (1) is the Zeeman energy.

The minimization of Eq. (1) with respect to φ_1 and φ_2 angles gives the equilibrium orientations of Ni magnetic moments. The type of the resulting magnetic structure depends on the signs and values of K_{Ni_1} and K_{Ni_2}. At $K_{\mathrm{Ni}_1}>0$ and $K_{\mathrm{Ni}_2}<0$ the Ni magnetic moments lie in the a-b plane as shown in Fig. 9. According to this arrangement each Ni subsystem is weakly ferromagnetic and these weakly ferromagnetic moments are oriented antiparallel to each other being aligned along the b axis. Therefore, the resulting magnetic structure of $Ni(HCOO)_2\cdot 2H_2O$ is a weakly ferrimagnetic one. The reversal of K_{Ni_1} and K_{Ni_2} signs results in a 90° rotation of the magnetic structure in the a-b plane. Below we consider a magnetic structure shown in Fig. 10.

Assuming that the crystal-field energy for Ni ions is much smaller than the energy of the exchange interaction, deviations from the antiparallel alignment will be small. In Ni_1 and Ni_2 subsystems these deviations will be denoted ε and δ, correspondingly (see Fig. 10). The minimization of free energy given by Eq. (1) at $H=0$ allows to obtain the deviations of magnetic moments ε and δ from antiparallel alignment within both Ni_1 and Ni_2 subsystems:

$$\varepsilon=-\frac{m(q_1\sin\psi_1-q_2\sin\psi_2)+2q_1q_2\sin\psi_1\cos\psi_2}{2[m(2+q_1\cos\psi_1+q_2\cos\psi_2)+2q_2(2\cos\psi_2+q_1\cos\psi_1\cos\psi_2)]}, \tag{2}$$

$$\delta=\frac{m(q_1\sin\psi_1-q_2\sin\psi_2)+2q_2(2\sin\psi_2+q_1\cos\psi_1\cos\psi_2)}{2[m(2+q_1\cos\psi_1+q_2\cos\psi_2)+2q_2(2\cos\psi_2+q_1\cos\psi_1\cos\psi_2)]}. \tag{3}$$

The angles ψ_1 and ψ_2 are the angles between axes of anisotropy within Ni_1 and Ni_2 subsystems, $q_1=K_{\mathrm{Ni}_1}/2IM_1^2$, $q_2=K_{\mathrm{Ni}_2}/2IM_1^2$, and $m=M_1/M_2$. The resulting weak ferrimagnetic moment in this model is

$$M_{total}=M_1(\varepsilon+m\delta)/2 \tag{4}$$

or taking into account the expressions for ε and δ,

$$\begin{aligned}M_{total}=&\frac{M_1m^2(q_1\sin\psi_1-q_2\sin\psi_2)}{4[m(2+q_1\cos\psi_1+q_2\cos\psi_2)+2q_2(2\cos\psi_2+q_1\cos\psi_1\cos\psi_2)]}\\&-\frac{M_1m(q_1\sin\psi_1+3q_2\sin\psi_2+2q_1q_2\cos\psi_1\cos\psi_2)}{4[m(2+q_1\cos\psi_1+q_2\cos\psi_2)+2q_2(2\cos\psi_2+q_1\cos\psi_1\cos\psi_2)]}\\&-\frac{M_12q_1q_2\sin\psi_1\sin\psi_2}{4[m(2+q_1\cos\psi_1+q_2\cos\psi_2)+2q_2(2\cos\psi_2+q_1\cos\psi_1\cos\psi_2)]}.\end{aligned} \tag{5}$$

This formula describes the evolution of the weak magnetic moment of $Ni(HCOO)_2\cdot 2H_2O$ with temperature. To calculate the temperature dependence of M_{total}, the $M_1(T)$ and $M_2(T)$ dependencies as well as $K_{\mathrm{Ni}_1}(T)$ and $K_{\mathrm{Ni}_2}(T)$ dependencies should be used. The temperature dependencies of molar sublattice magnetizations M_1 and M_2 can be calculated within the exchange approximation through the corresponding Brillouin functions B_S,

$$M_1=gS\mu_BN_AB_S[gS\mu_BI(4M_1+2M_2)/k_BT], \tag{6}$$

$$M_2=gS\mu_BN_AB_S[gS\mu_BI(2M_1)/k_BT], \tag{7}$$

where $S=1$ is a spin of Ni^{2+} ions and N_A is Avogadro's number.

The constants of single-ion anisotropy change with temperature as follows:[30]

$$K_{\mathrm{Ni}_1}(T)=K_{\mathrm{Ni}_1}(0)\hat{I}_{5/2}\{L^{-1}[M_1(T)]/M(0)\}, \tag{8}$$

$$K_{\mathrm{Ni}_2}(T)=K_{\mathrm{Ni}_2}(0)\hat{I}_{5/2}\{L^{-1}[M_2(T)]/M(0)\}, \tag{9}$$

where $\hat{I}_{5/2}$ is a normalized Bessel function; L^{-1} is an inverse Langevin function; $K_{\mathrm{Ni}_1}(0)$, $K_{\mathrm{Ni}_2}(0)$, and $M(0)$ are single-ion anisotropy constants; and the magnetic moment at $T=0$ K.

Equations (6) and (7) give the following formulas for the Néel temperature:

$$T_N=2CI(\sqrt{2}+1), \tag{10}$$

where $C=g^2S(S+1)N_A\mu_B^2/3k_B$.

The paramagnetic susceptibility above the Néel point T_N in this model is

$$\chi_{para}=\frac{C}{T+4CI-4C^2I^2/T}. \tag{11}$$

Clearly, the χ_{para} deviates from the Curie-Weiss law at lowering temperature, reflecting the existence of two different magnetic subsystems in $Ni(HCOO)_2\cdot 2H_2O$. Equation (11) represents a simplified expression for paramagnetic susceptibility of the ferrimagnet (Néel's law). The simplification arises from the facts that both magnetic subsystems are constituted by the same ions and the exchange interaction within one of them is absent. The inverse paramagnetic susceptibility becomes zero at

$$\Theta'=2CI(\sqrt{2}-1). \tag{12}$$

In exchange approximation it is possible also to calculate the molar transverse magnetic susceptibility in the magnetically ordered state, i.e., below the Néel point,

$$\chi_{antif}=\frac{N_A(1+m)^2}{16I}. \tag{13}$$

Note that the temperature dependence of χ_{antif} is not trivial. It increases at lowering temperature due to the fact that the Ni_2 subsystem itself is paramagnetic in the absence of exchange interaction with the Ni_1 subsystem.

V. DISCUSSION

The experimental data available for $Ni(HCOO)_2\cdot 2H_2O$ can be compared with results of analytical and numerical calculations within the model proposed. Equation 10 allows to estimate the exchange interaction coefficient $I=3.9$ K from the value of the Néel temperature $T_N=15.5$ K.[31] Using this value of the exchange interaction coefficient the paramagnetic Curie temperature extrapolated from the high-temperature region is $\Theta=-4CI=-12.7$ K [see Eq. (11)], which is close to the experimentally determined value $\Theta=-15.5$ K. The temperature dependence of inverse paramagnetic susceptibility χ_{para}^{-1} calculated from Eq. (11) is shown in Fig. 8 by the dotted line. This theoretical dependence coincides with the experimental dependence in a broader temperature range than that of the Curie-Weiss law. The extrapolated value $\Theta'=3.6$ K is close to the theoretical estimate $\Theta'=2.6$ K.

The temperature dependencies of sublattices magnetization $M_1(T)$ and $M_2(T)$ were calculated from Eqs. (6) and (7). These dependencies along with the ratio $m(T)=M_1(T)/M_2(T)$ are plotted in Fig. 11. The difference in behavior of Ni_1 and Ni_2 subsystems is clearly seen from these dependencies. While the magnetization of the Ni_1 subsystem closely follows the behavior of the typical ferromagnet or antiferromagnet, the magnetization of the Ni_2 subsystem strongly deviates from this behavior. This is due to the fact that the exchange interaction within the Ni_2 subsystem does not exist and it orders magnetically only due to the exchange interaction with the Ni_1 subsystem.

The temperature dependence of transverse magnetic susceptibility χ_{antif} in the magnetically ordered state calculated from Eq. (13) is in correspondence with experimental data, as shown in Fig. 7. To make this comparison we assumed that the magnetic susceptibility of the powder sample at high magnetic field is that of the transverse the magnetic susceptibility of the single crystal. The theoretical and experimental curves are qualitatively similar, but experimentally found values are somewhat larger than the calculated ones. This can be due to the presence of a small amount of paramagnetic impurities in the sample.

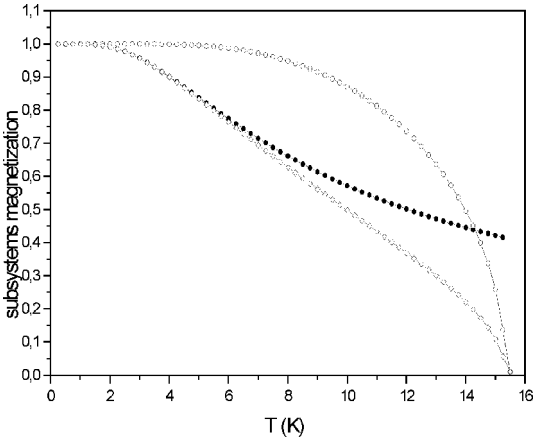

FIG. 11. The temperature dependencies of reduced magnetizations $M_1(T)/M(0)$ of Ni_1 (○) and $M_2(T)/M(0)$ of Ni_2 (◇) sublattices along with the ratio $m(T)=M_1(T)/M_2(T)$ (●).

The physical scenario for the appearance of the compensation point at temperature dependence of weak magnetization of $Ni(HCOO)_2\cdot 2H_2O$ in the model presented is as follows. At cooling below the Néel temperature the weak magnetization of the Ni_1 subsystem exceeds that of the Ni_2 subsystem. This occurs because $M_1(T)$ dependence is much steeper than $M_2(T)$ dependence in the vicinity of T_N. At further cooling, the values of Ni_1 and Ni_2 sublattice magnetization approach each other. If magnetic anisotropy in the Ni_2 subsystem is ''larger'' than that of the Ni_1 subsystem, at low temperatures the weak magnetization of the Ni_2 subsystem will prevail. The temperature dependence of the weak ferrimagnetic moment M_{total} is determined not only by sublattice magnetizations $M_1(T)$ and $M_2(T)$ but also by single-ion anisotropies $K_{Ni_1}(T)$ and $K_{Ni_2}(T)$ [see Eq. (5)]. To determine M_{total} vs T dependence the absolute values of $K_{Ni_1}(0)$ and $K_{Ni_2}(0)$ were calculated from the values of $M_{total}=0$ at a compensation temperature T^* and M_{total} at saturation of both Ni_1 and Ni_2 magnetic subsystems at $T=0$ K, i.e., at $m=1$. Taking into account that the experimental data were obtained from a powder sample we will assume that the weak ferromagnetic moment observed corresponds roughly to one-third of that of M_{total}. At $T=0$ K, the anisotropy constants $K_{Ni_1}(0)=6.43\times 10^8$ erg/mole and $K_{Ni_2}(0)=-1.86\times 10^8$ erg/mole. $M_{total}(T)$ calculated from Eq. (5) is shown in Fig. 4. Good correspondence between experimental and theoretical curves is clearly seen.

The field dependencies of magnetization of $Ni(HCOO)_2\cdot 2H_2O$ at low temperatures are nonlinear and differ from that expected for a typical two sublattice antiferromagnet.

The calculations within the framework of our model indicate that this behavior is due to the presence of two nonequivalent interacting magnetic subsystems. The theoretical M_{total} vs H dependence for H parallel to the b axis of the single crystal at $T=2$ K is represented in the inset to Fig. 3. Though the experimental data are obtained from the powder sample and calculations are performed for a single crystal, the nonlinearity of both M vs H curves is clearly seen.

VI. CONCLUSION

This paper presents the results of experimental and theoretical studies of magnetic properties of the nickel (II) formate dihydrate $Ni(HCOO)_2 \cdot 2H_2O$. At $T_N=15.5$ K this compound undergoes a transition to a magnetically ordered state, exhibiting peculiar magnetic properties: a weak spontaneous ferromagneticlike moment, compensation point, and the phenomenon of magnetization reversal. It is concluded that $Ni(HCOO)_2 \cdot 2H_2O$ is a weak ferrimagnet at low temperatures.

Weak ferrimagnetism arises from the competition of weak ferromagnetic moments of two nonequivalent canted antiferromagnetic Ni_1 and Ni_2 subsystems. The deviations from antiparallel alignment of magnetic moments within these subsystems are caused by single-ion anisotropy. The compensation point is due to the difference in temperature dependencies of weak ferromagnetic moments of Ni_1 and Ni_2 subsystems.

In the framework of molecular-field approximation a simple model is proposed which accounts for the main features of the magnetic behavior of this compound. It describes qualitatively the temperature dependence of the weak ferrimagnetic moment and magnetic susceptibility both above and below the Néel temperature.

Some quantitative disagreement of calculated results with experimental data can be due to the fact that the measurements were done with powder samples, so the obtained data are averaged over different crystallographic directions. The limitations of the model itself are mentioned above.

ACKNOWLEDGMENTS

The authors acknowledge useful discussions with Professor Y. Ueda and the assistance of Dr. T. Uchimoto and Mr. T. Okuyama in numerical calculations. This work was supported by the Netherlands Foundation for the Support of Science (NWO) through Project No. 008-012-047.

*On leave from Low Temperature Physics and Superconductivity Department, Moscow State University, Moscow 119992, Russia. Electronic address: vasil@lt.phys.msu.su

[1] S. Krupicka, *Physik der Ferrite und der Verwandten Magnetischen Oxide* (Academia, Prague, 1973).
[2] S. Chikadzumi, *Physics of Ferromagnetism*, 2nd ed. (Oxford University, New York, 1997).
[3] N. Menyuk, K. Dwight, and D.G. Wickham, Phys. Rev. Lett. **4**, 119 (1960).
[4] N. Sakamoto and Y. Yamaguchi, J. Phys. Soc. Jpn. **17** (B1), 276 (1962).
[5] C. Mathoniere, C.J. Nuttall, S.G. Carlong, and P. Day, Inorg. Chem. **35**, 1201 (1996).
[6] N. Re, E. Gallo, C. Floriani, H. Miyasaka, and N. Matsumoto, Inorg. Chem. **35**, 5964 (1996).
[7] S.I. Ohkoshi, T. Iyoda, A. Fujishima, and K. Hashimoto, Phys. Rev. B **56**, 11 642 (1997).
[8] S.I. Ohkoshi, Y. Abe, A. Fujishima, and K. Hashimoto, Phys. Rev. Lett. **82**, 1285 (1999).
[9] A. Bhattacharjee, R. Feyerherm, and M. Steiner, J. Phys. Soc. Jpn. **68**, 1679 (1999).
[10] O. Cador, M.G.F. Vaz, H.O. Stumpf, and C. Mathoniere, J. Magn. Magn. Mater. **234**, 6 (2001).
[11] N. Shirakawa and M. Ishikawa, Jpn. J. Appl. Phys., Part 2 **30**, L755 (1991).
[12] A.V. Mahajan, D.C. Johnston, D.R. Torgeson, and F. Borsa, Phys. Rev. B **46**, 10 966 (1992).
[13] L. Néel, Ann. Phys. (Leipzig) **3**, 137 (1948).
[14] T. Moriya, in *Ferromagnetism*, edited by G.T. Rado and H. Suhl (Academic, New York, 1963), Vol. 1.
[15] I. Dzyaloshinsky, J. Phys. Chem. Solids **4**, 241 (1958).
[16] T. Moriya, Phys. Rev. **117**, 635 (1960).
[17] T. Moriya, Phys. Rev. **120**, 91 (1960).
[18] Y. Ren, T.T.M. Palstra, D.I. Khomskii, E. Pellegrin, A.A. Nugroho, A.A. Menovsky, and G.A. Sawadzky, Nature (London) **396**, 441 (1998).
[19] Y. Ren, T.T.M. Palstra, D.I. Khomskii, A.A. Nugroho, A.A. Menovsky, and G.A. Sawadzky, Phys. Rev. B **62**, 6577 (2000).
[20] A.M. Kadomtseva, A.S. Moskvin, I.G. Bostrem, B.M. Vanklin, and N.A. Hafizova, Sov. Phys. JETP **72**, 2286 (1977).
[21] K. Yamagata, J. Phys. Soc. Jpn. **22**, 582 (1967).
[22] R.D. Pierce and S.A. Friedberg, Phys. Rev. **165**, 680 (1968).
[23] J. Skalyo, Jr., G. Shirane, and S.A. Friedberg, Phys. Rev. **188**, 1037 (1969).
[24] K. Takeda and K. Kawasaki, J. Phys. Soc. Jpn. **31**, 1026 (1971).
[25] G.R. Hoy, S. de S. Barros, F. de S. Barros, and S.A. Friedberg, J. Appl. Phys. **36**, 936 (1965).
[26] P. Burlet, E.F. Bertaut, G. Roult, A. de Combarieu, and J.J. Pillon, Solid State Commun. **7**, 1403 (1969).
[27] R.D. Pierce and S.A. Friedberg, Phys. Rev. B **3**, 934 (1971).
[28] K. von Krogmann and R. Mattes, Z. Kristallogr. **118**, 291 (1963).
[29] J.B. Goodenough, *Magnetism and the Chemical Bond* (Wiley, New York, 1963).
[30] H. Callen and E. Callen, J. Phys. Chem. Solids **27**, 1271 (1966).
[31] The exchange interaction parameter $I=3.9$ K is nearly two times less than the estimate given for the interlayer exchange interaction parameter in Ref. 24. This arises from the difference in definitions of the Hamiltonians and is connected also to the fact that interlayer exchange interactions are taken into account in the present work.